Proceedings of ASME:1999 NHTC

33rd NATIONAL HEAT TRANSFER CONFERENCE

AUGUST 15–17, 1999

Albuquerque, New Mexico

NHTD99-34

Thermal FEA and Validation

Savithri Subramanyam
Material & Controls Group
Texas Instruments, Inc. Attleboro, Massachusetts

Keith E. Crowe
Material & Controls Group
Texas Instruments, Inc. Attleboro, Massachusetts

Abstract

This paper discusses use of state-of-the-art tools that are valuable in understanding the operation of thermally driven devices. Judicious use of these tools results in shortening the cycle time when applied earlier in the design process. Use of FEA allows one to solve problems with highly non-linear physics and material properties, field coupling, and complex geometry. Thermal FEA coupled with infrared imaging and wind tunnel testing for validation has proven to be a powerful tool in the early stages of design. The two methodologies complement one another and are more powerful in unison than when used individually. Examples of the application of these tools to commercial products are given.

Introduction

Predicting the heat transfer in a process can be done by two main methods: theoretical calculation and experimental evaluation. Each method has its advantages and disadvantages, but utilizing both techniques wherever possible provides a dynamic combination. The methods complement each other, for the amount of experimentation can be reduced significantly if supplemented by computation. The relative number of computational vs. experimental investigations depends on the objective of the prediction, the physics of the problem, and other constraints such as turnaround time and cost. It is a common practice in industry to rely solely on either experimentation or computation to achieve the above objectives. However, a judicious combination of both methodologies provides the most reliable prediction for the majority of the thermal problems.

NOMENCLATURE

Table 1: Nomenclature

I	Electric Current	A
J	Current Density	A/m^2
R	Electrical Resistance	O
V	Electrical Potential	V
k	Thermal conductivity	W/m-C
q	Internal Heat Generation	W/m^3
a	Thermal diffusivity	m^2/s
T	Temperature	C
?	Electrical Resistivity	O-m
t	Time	s

COMPUTATIONAL LABORATORY STRUCTURE

The basic structure of the computational facility of our analysis group at Material and Controls Group (M&C) of Texas Instruments has been described in detail (Mandeville and Rolph). Our thermal/fluid FEA architecture segregates the discrete tasks and utilizes software specifically designed for that task. In the model generation stage or *pre-processing* PATRAN (MacNeil-Schwendler Corporation) is used to define the continuum, finite element mesh, loads/boundary conditions, and element properties. In most 3-d analysis, the data preparation can consume 70-80% of the labor hours required. Once the model is set up, it is then executed using the appropriate analysis package.

The analysis packages used in our thermal analysis laboratory are ADINA-T (ADINA R&D) and FIDAP (FLUENT Inc.). Within each finite element, the dependent variables such as velocity, pressure, and temperature are interpolated by functions of compatible order. These are done in terms of undetermined values at nodal points. For most analysis, higher order 20 node hexahedral elements are employed. These elements can give accurate solutions with surprisingly few elements, particularly for thermal conduction problems. Element assemblage, where interelement continuity is enforced, results in discrete representation of the continuum formulation. The solver then computes a steady state solution or the transient response using explicit or implicit time integration techniques.

Typically, the solution of such non-linear sets of matrix equations is the most time consuming stage with respect to computer resources. This could account for 80% of the resources needed for a fully coupled non-linear analysis. Examples of such situations occur when momentum and energy equations are coupled not only by the convective and viscous terms, but also the temperature (or concentration) field, like the buoyancy term. In the case of turbulent flows, there are two more additional transport equations that are strongly coupled to the momentum equations.

One of the key features of this facility is that all analysis codes are licensed in source. This allows the user to incorporate features into the package that are proprietary to the needs of the customer. For example, ADINA-T is strictly a three dimensional thermal analysis code. An inherent feature to the majority of our devices such as circuit breakers and motor protectors is Joule (or the I^2R) heating. ADINA-T was modified (Rolph) to incorporate this type of heat loading. The coupled thermo-electric problem is governed by the set of simultaneous equations:

$$\nabla^2\theta = \frac{1}{\alpha}\frac{\partial\theta}{\partial\tau} + \frac{1}{k}\left(\vec{\nabla}V\cdot\left(\frac{1}{\rho(\theta)}\vec{\nabla}V\right) + \dot{\Phi}_{other}\right) \quad (1)$$

$$\vec{\nabla}\cdot\left(\frac{V}{\rho(\theta)}\right) = \dot{J} \quad (2)$$

Bi-directional coupling occurs when (as is generally the case) electrical resistivity is a function of temperature. Solution of this set requires formation of the electrical (as well as thermal) conductivity matrices. Thus, the computational effort is twice that of the thermal problem alone. Highly non-linear resistivity can require significant iterations for convergence, however.

Results evaluation or *post-processing* is performed again using PATRAN (and FIPOST for CFD). Fundamental field variables such as the temperature, velocity and pressure as well as derived quantities such as heat flux, heat transfer coefficient, Reynolds number, mass flow rate, etc. are mapped onto the geometric model. In case of coupled electrical-thermal problems, mapping of voltage and current density are also important.

EXPERIMENTAL CAPABILITIES

The experimental facility has numerous capabilities most notably infrared (IR) imaging and wind tunnel testing. The infrared imaging technique provides one of the best methods for obtaining temperature fields. The unique feature of this method lies in the fact that it is a non-contact means of testing and hence is non-intrusive. Unlike the contact method of temperature measurements (ex. Thermocouples) that work by the principle of conduction, the non-contact method of temperature measurements uses the principles of radiation. Some of the advantages of using infrared imaging technique are:

1. Pictorial representation of the thermal interaction within various parts in the device.
2. No lag or response time issues as with contact methods. Real time recording of the event as fast as the capture rate of the camera.
3. Full field visibility.

4. Good post processing capabilities with the information recorded to trouble shoot process/design problems.

The major drawback of this method lies in the fact that a high emissivity is required to get an accurate correlation between radiation and temperature. In many cases it is possible to coat the object under observation with a flat black paint. In such cases, the object closely approximates a blackbody whose total heat flow is connected with radiation effects of absorption or emission. This object radiates across the entire infrared spectrum. In cases where it is not possible to paint the object black, one must calibrate the object's radiation measurement to a measurement that is known. When these measures are taken properly, IR temperature measurements are accurate to within a degree C.

1. Emissivity variances within a device can lead to spurious radiation. Hence accuracy is largely dependent on emissivity and absence of any reflections.
2. The object of interest may not be accessible to view with the IR system.
3. Inadequate proximity to the object may result in inaccurate measurements.

Despite the drawbacks, IR imaging is an excellent tool to complement the efforts of thermal modeling as it provides a map of the temperature field that should match the FEA model in shape even though the actual numbers may differ due to computational and/or experimental errors. If the two solution fields map well, then the physics of the problem has been captured in the model and further modification or optimization of a design can be done with greater confidence.

One necessity to validating thermal performance of electronic systems under forced-convection is wind-tunnel testing. The thermal resistance of air-cooled electronic devices depends strongly on air flow velocity. Accurate measurement and control of airspeed is vital. The wind tunnel that we currently use is made of Plexiglas for ease of flow visualization. The flow is controlled using hot-wire anemometry. There are flow straighteners and turbulence dampers. Instrumentation and wiring ports are on the side walls to minimize flow disturbance. There are two-fan trays that can support flow speeds from 0-2000 linear feet per minute. The test section was modified to have an IR window that will allow us to capture the temperature distribution of the test piece under forced convection. This again is an important tool to validate the CFD models to obtain the map of the temperature solution on the heat sinks. The shape of the field relates to important information on the performance of the heat sinks.

As mentioned earlier, capturing the true physics of the problem requires that any non-linearity in problem must be taken into account. One of the major sources of non-linearity in modeling motor-protectors or circuit-breakers is the variation of properties as a function of temperature. Experience has shown that ignoring such variations could result in predictions that are in error by greater than 25%. Characterization of material properties is routinely performed to accompany most analyses. Such efforts have usually resulted in excellent agreement with the analysis and tests.

EXAMPLES ON THE DEPLOYMENT OF THE THERMAL TOOLS

Analytical results of some applications will be presented next. The results were obtained using the tools outlined above.

Example 1: Transient conduction with Joule heating

The problem of protecting motor windings from high temperatures is very important to motor manufacturers, the motor user, and the general public. In the early days, the motors did not have adequate protection against overheating. It was mainly done with fuses, and the shortcomings of the fuses led to other types of protection. Today, one of the most common ways is to use some sort of a thermostatic device such as a bimetallic strip, together with a heater coil, which is then hermetically sealed. Figure 1 shows an example of such a device. In this class of protectors, the thermal element is responsive to both the flow of motor current through the protector and the ambient temperature surrounding the protector.

These device must satisfy two extremes of operating performance: The ultimate trip (normal operating conditions) and short-time trip (locked rotor conditions). In ultimate trip, the actual current to trip the device depends strongly on the ambient temperature and this current decreases with increasing ambient temperature for a given device. Computational analysis of the ultimate trip conditions is difficult, involving detailed creation of all the components within the protector, including the gaseous environment. The analysis is the solution of coupled electrical, thermal, and convection (and perhaps radiation) equations with highly nonlinear terms.

In short-time trip, the line current enters the protector and flows through the bimetallic disk often mounted adjacent to a heater (used for auxiliary heating of the disc). During the "on" time, the electrical contacts are closed and the disk heats up by virtue of I^2R heating. When the disk attains it opening temperature, the disk snaps and breaks open the contacts. This is called the short-time trip or locked rotor condition trip. The motor is disconnected from the line (until the system cools to the reset temperature). During this very short time, the mass of the motor, the effect of ambient, and radiation from the motor have very little effect on the heating of the disc (adiabatic heating). Figure 2 shows the temperature

results under locked rotor conditions while Fig. 3 shows the voltage drop in the device. The voltage field provides an additional validation point, since voltage measurement is typically simple and accurate.

A prototype was built and tested to validate the FEA using IR imaging. Figure 4 shows the temperature field of the device when viewed from the side. The frame rate of capture was set to 4 frames/sec. One interesting feature of the image is the hot spot seen between the disk and the movable contact. FEA model for short time trip analysis does not include the heat generation due to contact/contact interface. The standard practice for such models is to model the device (1/2 model if symmetrical as in Fig. 2) with the top of the movable contact grounded to zero and current into the pin. In the majority of cases this type of analysis gives excellent correlation with the time and the temperature to trip for a given current. Most of the heat generation occurs in the bimetal itself (or sometimes-additional heat in the auxiliary heater) and thus the physics is reasonably well captured by this representation.

Further tests were done with the standard time-check board (which can deliver a precise high current) to collect data on a larger number of samples which is more cost effective than using IR for getting statistical distribution. The error in trip time between the FEA and the test was computed. The FEA "trip time" was based upon the time required for the disc temperature to reach a specified threshold, while the test data was represented by the average trip time, accurate to well within 0.5%. Analysis error was calculated to be 1.8% for low current and 4.8% for high current cases.

Once a model has been validated, then a whole family of curves can be generated using various combinations of disc/heater materials and/or geometry for various ratings. The time savings for this effort vs. conventional prototyping is enormous.

Example 2: Highly non-linear, coupled problems

This example shows the simulation of a highly non-linear system where the electrical resistivity changes as a function of temperature as well as electric field. A typical curve for such a class of material system called the PTC (positive temperature coefficient) is shown in Fig. 5. The knee (Curie point) portion of the curve can be changed by composition/processing techniques. The slope of the R-T curve beyond the Curie point determines the operating or *switch* temperature of the device. From Fig. 5, it is clear that the device shows a self-limiting power condition when heated beyond the Curie point. Further voltage increase can give rise to PTC heating where the "end point" is exceeded. The "end point" refers to the ability of the device to withstand a pulsed voltage with some safety margin without approaching the condition of thermal runaway if placed in a powered condition.

In performing the FEA, the actual R-T curve was input with appropriate coefficients for electric field sensitivity. The mathematical model for this is proprietary. A 2-d axi-symmetric model of the pill with inset metallic contact was modeled. The transient response of the pill was calculated.

Prototype failures were observed to occur either through edge arcing or edge cracking. Figures 6 and 7 show the temperature and the voltage drop, across a PTC pill for a certain application. The thermal analysis is an important tool to detect potential hot spots or thermal runaway areas that could lead to failure modes. Mechanical stress analysis using ADINA (ADINA R&D) was performed (courtesy Rolph III, W.D.) using the calculated temperature field as a loading. Figure 8 shows the maximum principal stress field which is consistent with the results of failure analysis.

Example 3: Steady state conjugate heat transfer (CFD)

Higher power densities in electronic modules now routinely require some form of active cooling; typically a solid heat sink with forced air cooling. Package size limitations in both service and manufacture require that designs be effective and efficient, which means that performance predictions are critical. One of the final manufacturing steps for certain chips is the burn-in where chips are powered up for an extended time for stabilization and to identify short life devices. The M&C group manufactures burn-in test sockets (BITS) for chip manufacturers which incorporates an integral heat sink customized to the product and its processing. Figure 9 shows an example of such a socket. These applications require that sockets occupy only a small envelope and that chip temperatures be kept below critical levels. Predictive tools for design are critical to the process.

Historically, the approach has been to model the heat sink design using a lumped element FEA. Here, the heat transfer coefficient is estimated from well know correlations e.g. flat plate, and applied uniformly to heat transfer surfaces. Designs that give reasonable performance were rapidly prototyped and wind tunnel tested under conditions simulating the actual environment. This process has been effective to this point as is illustrated in the following example.

A nine fin heat sink is to dissipate chip power at an overall resistance of 7 C/W which includes the die/heat sink interface resistance. A design of aluminum heat sink was proposed and analyzed. With an estimated h of 0.030 W/in^2 C, the thermal FEA predicted 5.5 C/W as can be seen in the thermal field of Fig. 10. With an assumed interface resistance of 1 C/W the analysis predicts this design will meet spec. Wind tunnel testing indicates a thermal resistance of 6.3 C/W. Typically it has been found that calculations are slightly conservative with respect to test results. This is likely due to a conservative approach taken to allowable heat transfer area. In fact all exposed surfaces will transfer heat to the ambient, only fins sides are allowed to transfer heat in the calculations.

Though this approach has served well from a practical standpoint, there are a number of deficiencies: a) the nature of the flow field and heat transfer coefficient distribution are not well known b) when the fin shapes deviate from standard plate, empirical relations for h may not exist c) it is not well suited to design optimization and d) it provides no insight on the issue of interface resistance. As product requirements become more aggressive, continued good predictions will require more sophisticated tools to understand the details of the heat transfer process better.
Current efforts work toward incorporating computational fluid dynamics (CFD) analysis to solve the conjugate heat transfer problem. Figure 11 shows the flow field around a single fin model of a typical heat sink. A significant, flow by-pass (out the top) occurs, which shows that much less flow actually passes between the fins than the lumped model assumes. A single fin analysis is adequate for calculating the Nusselt number distribution, which can be applied to a multi-fin sink in lumped manner, however a full model CFD would be preferred. Model size and run time in these inherently non-linear problems has precluded this approach to date. We are currently working toward ramping up capabilities to routinely solve these problems.

IR imaging has also provided some insight on the performance of these products. We have recently integrated the IR capability with wind tunnel testing. To this point quantitative comparison between the FEA and IR thermal fields has not been done, but qualitative results have been revealing. Figure 12a shows a thermograph looking down on a heat sink at steady state with air flow moving left to right. Due to air heat up, a smooth increase in fin temperature occurs while moving to the right as expected. In Fig. 12b an abrupt temperature change occurs. The two half heat sinks latch separately, and it is clear the left heat sink has not made good thermal contact with the die, revealing the interfacial effect can be significant and very inconsistent. To this point interface resistance has been assumed a constant value based upon a limited data set. The increasingly aggressive performance requirements of the electronic cooling industry will require a better understanding of the interface and means to consistently lower its resistance.

Example 4: Coupled Thermal/Mechanical problems

The final example to illustrate the use of our computational/experimental tools in product development is a coupled thermal mechanical analysis with Joule heating. During the design stage of motor starter terminal assembly, it was found that regions of the terminal were experiencing excessively high stresses leading to fracture. It was known that the high stress location also experienced the maximum temperature in the assembly. An FEA was run to evaluate the potential for high thermally induced stresses in the component.

Initially, IR imaging was employed to understand the temperature field occurring during a high current transient. The IR thermograph shown in Fig. 13 indicates not only that the highest temperatures occur in the failure location, but that large gradients exist there as well. Evaluating the thermal stress field based upon the measured temperatures, although plausible is cumbersome. The strategy employed here was to compare measured thermal fields to thermal FEA results and use the calculated field as a load to the mechanical solver, ADINA.

Figure 14 shows the results of the thermal FEA. The field shows good similarity with the IR image and it was found that the maximum temperature rise is within 7%. Using the same finite element mesh, ADINA used the thermal results to compute the stresses at that time. Figure 15 shows the Von Mises stress field. The induced stresses are relatively low, in fact the stress is not maximum at the maximum temperature location. Thus it was learned that thermal stress was not a large factor in component failure. It was determined in a separate analysis that mechanical loading was chiefly responsible for the component fracturing. Given the agreement of the FEA and IR imaging, the part could be confidently redesigned to add material in the critical area to reduce maximum temperature and increase stiffness (reduce stress).

SUMMARY

The Thermal Analysis Laboratory at the Materials and Controls group of Texas Instruments has been constructed specifically to understand physical behavior of our products. Its mission is to provide insight on product performance and help engineers in their goal of reducing the design cycle. The facility has two main thrusts: computational and experimental. Each area provides validation for the other, which is crucial when analyzing systems and components that have coupled, non-linear physics. Effective use of both methodologies can reduce the number of required experiments and prototype cycles, as well reveal behavior that might go unnoticed if only one method is available.

Acknowledgments

The authors wish to thank Jack Brownlee of Texas Instruments for his outstanding support in performing the experiments which provided the data for the examples given here.

References

ADINA R&D, Inc. 71 Elton Ave., Watertown, MA 02172

FLUENT, Inc. 10 Cavendish Court, Centerra Resource Park, Hanover, NH 03766

MacNeil-Schwendler Corporation, 815 Colorado Blvd, Los Angeles, CA 90041

Mandeville, R.E. and Rolph III, W.D., "The design of a finite element facility based on ADINA", *ADINA Conference*, 1985

Rolph III, W.D., "Implementation of a Joule heating algorithm in ADINA-T", *Computers and Structures*, v. 26, n. 2, pp. 57-61, 1987

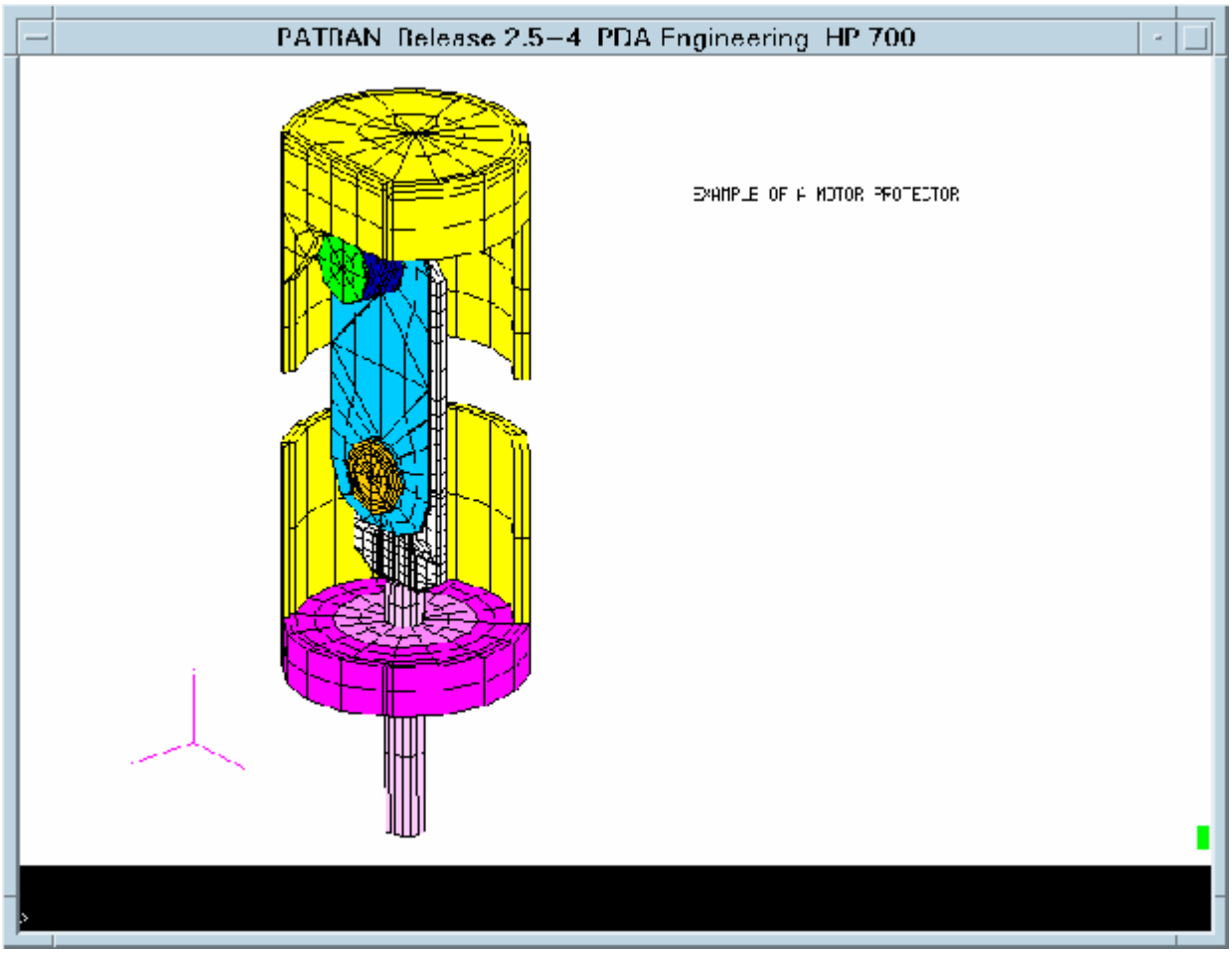

Figure 1: Example of a motor protector

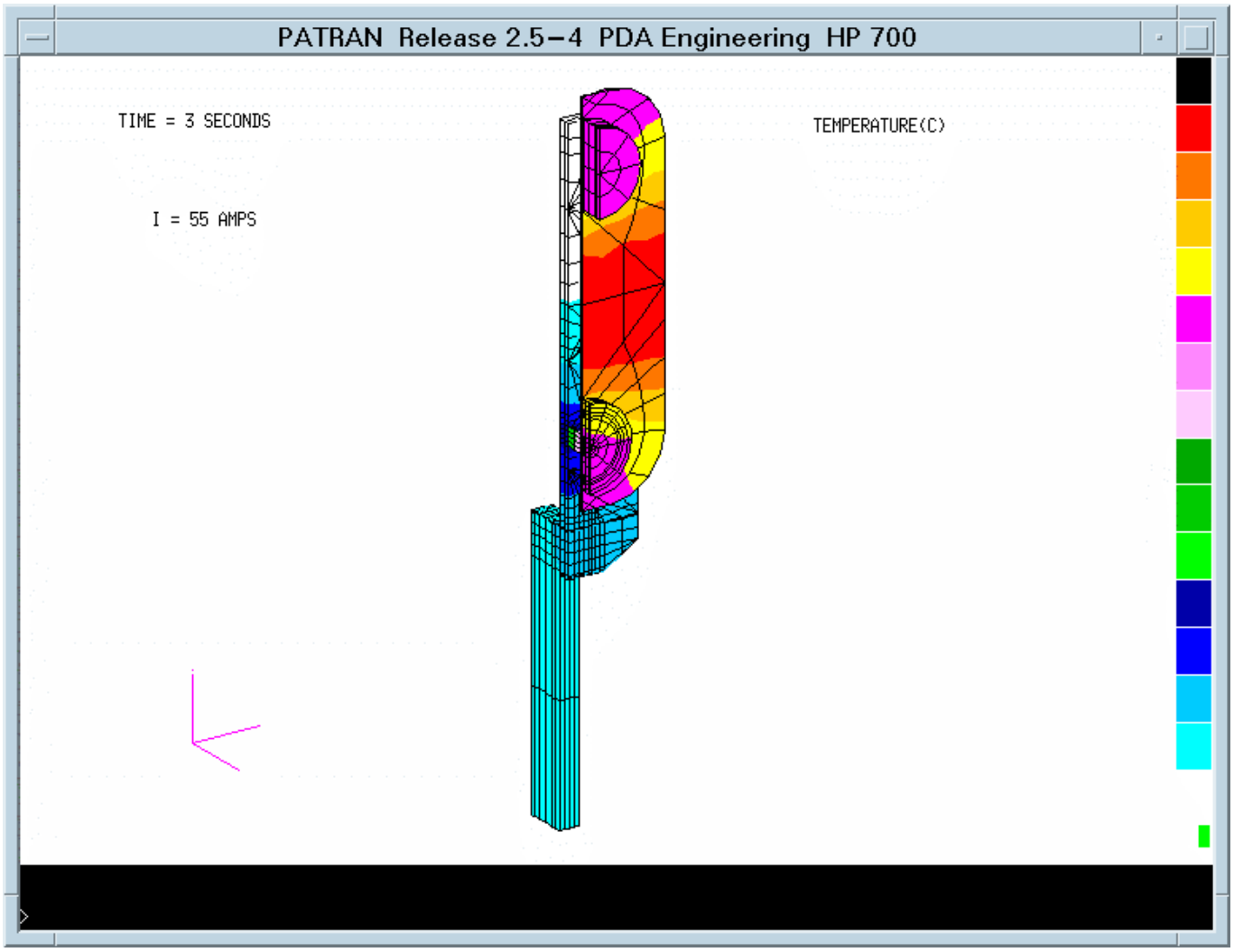

Figure 2: Temperature distribution for a given current and time.

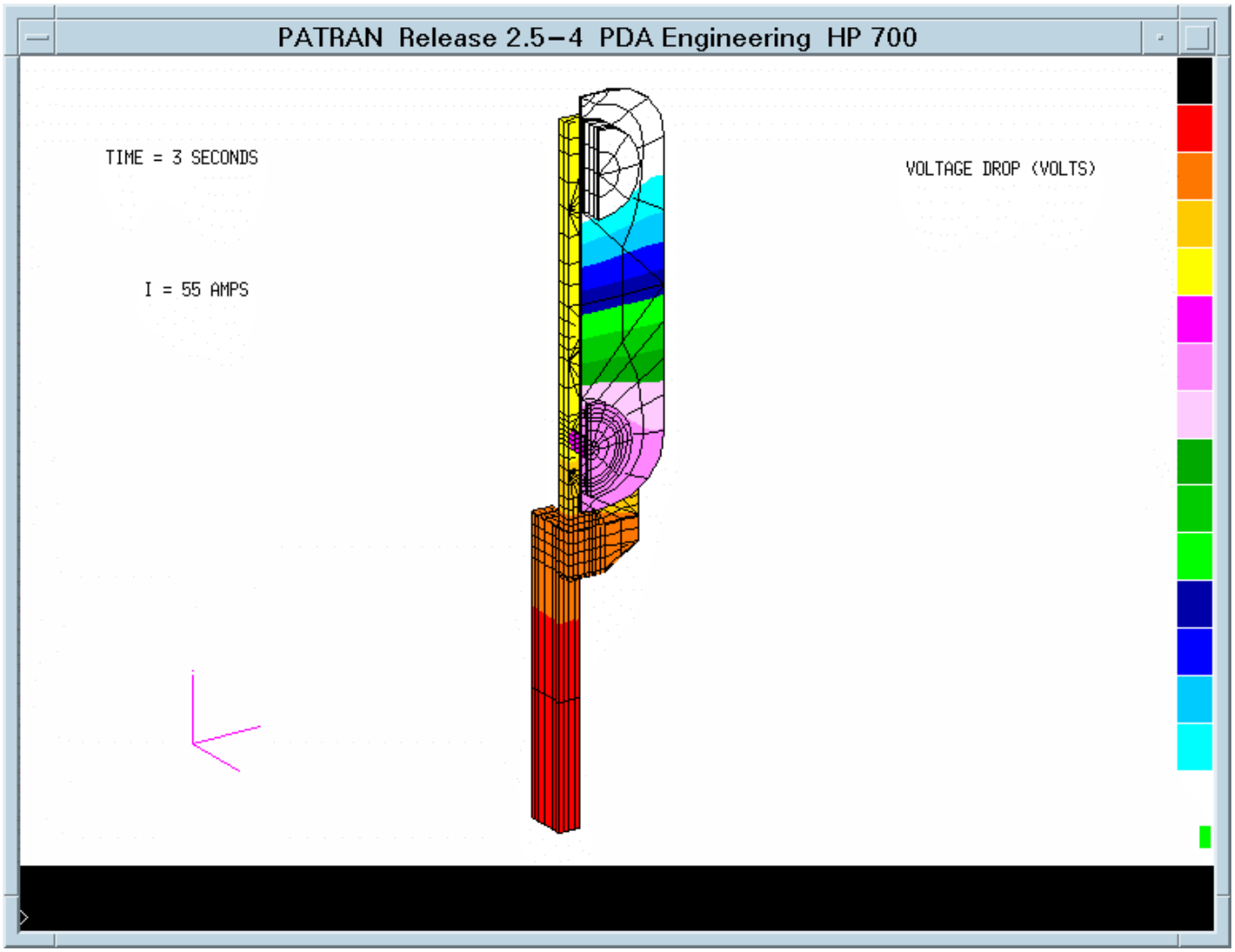

Figure 3. Voltage drop for a given current and time

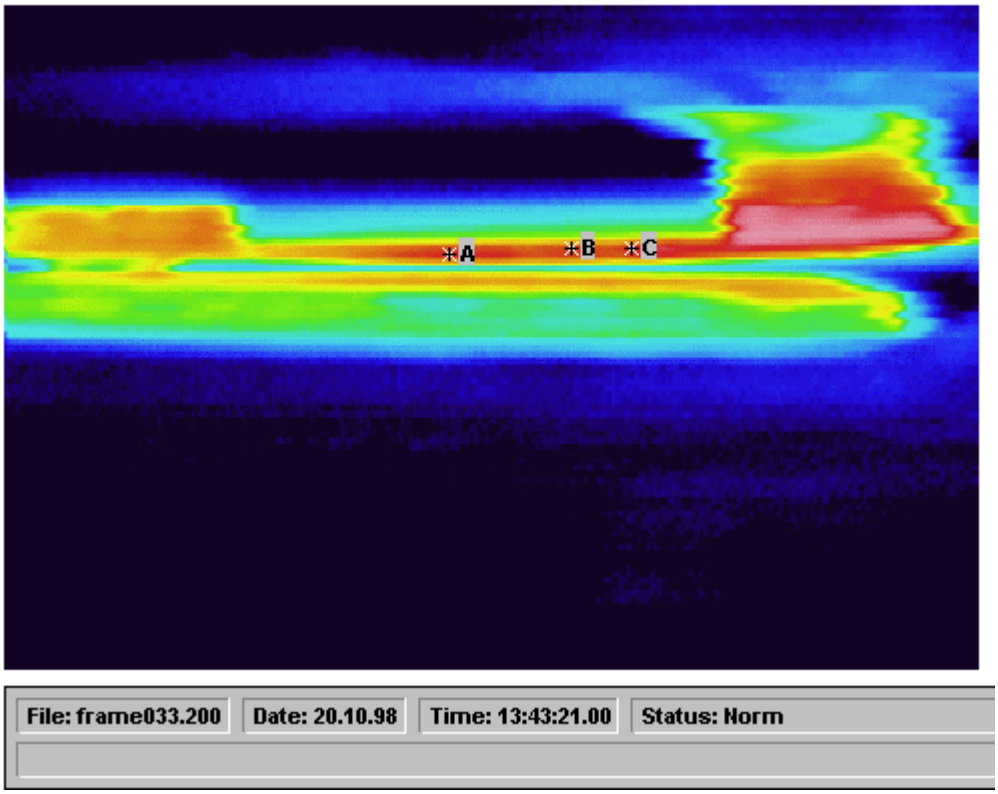

Figure 4: IR image of a device at an instant in time

Figure 5: Typical R-T curve for a PTC material

Figure 6. Temperature distribution in the pill.

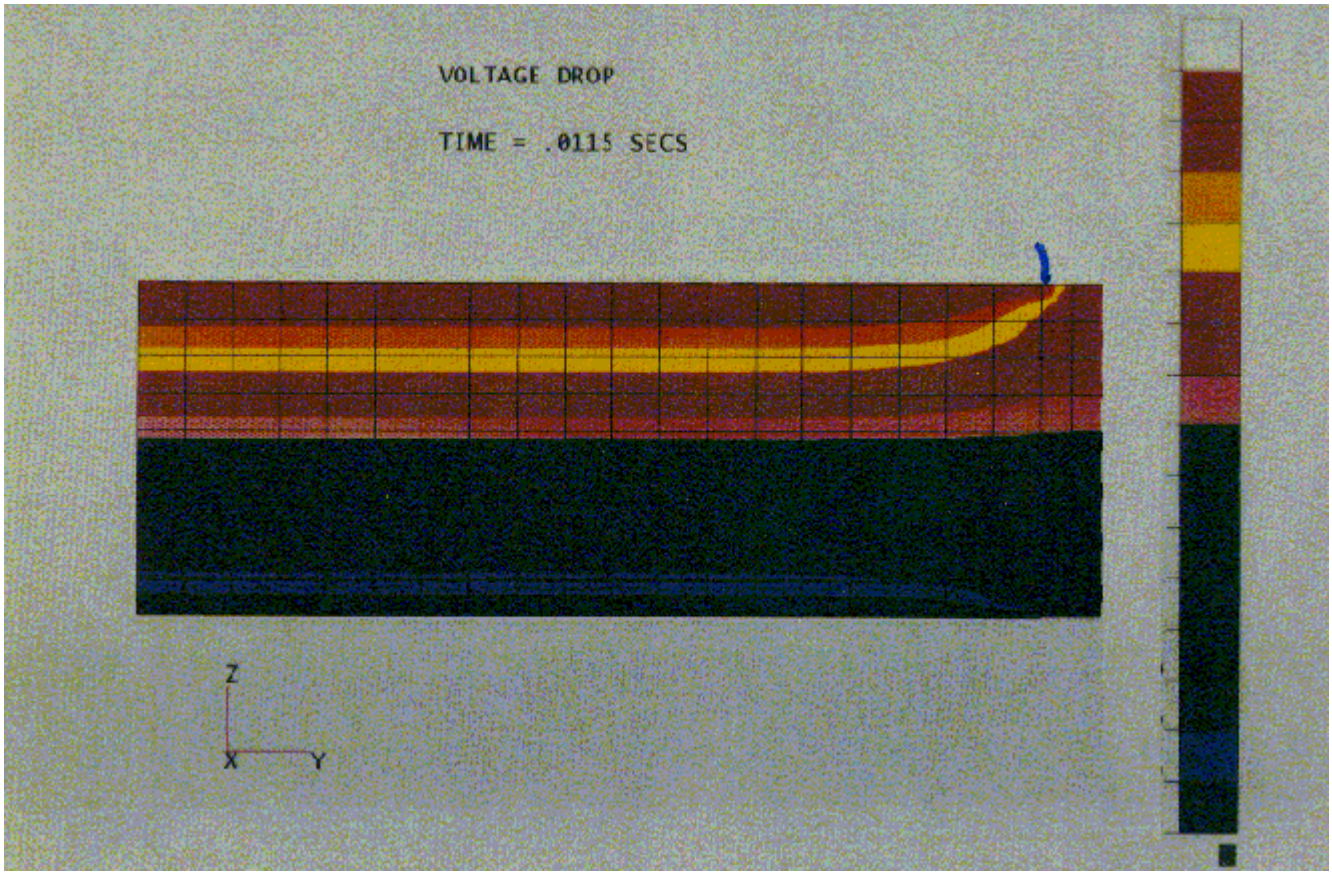

Figure 7. Voltage distribution in the pill.

Figure 8. Thermal stresses in the pill (Rolph III, W.D.)

Figure 9: Photograph of burn-in test socket with integral heat sink

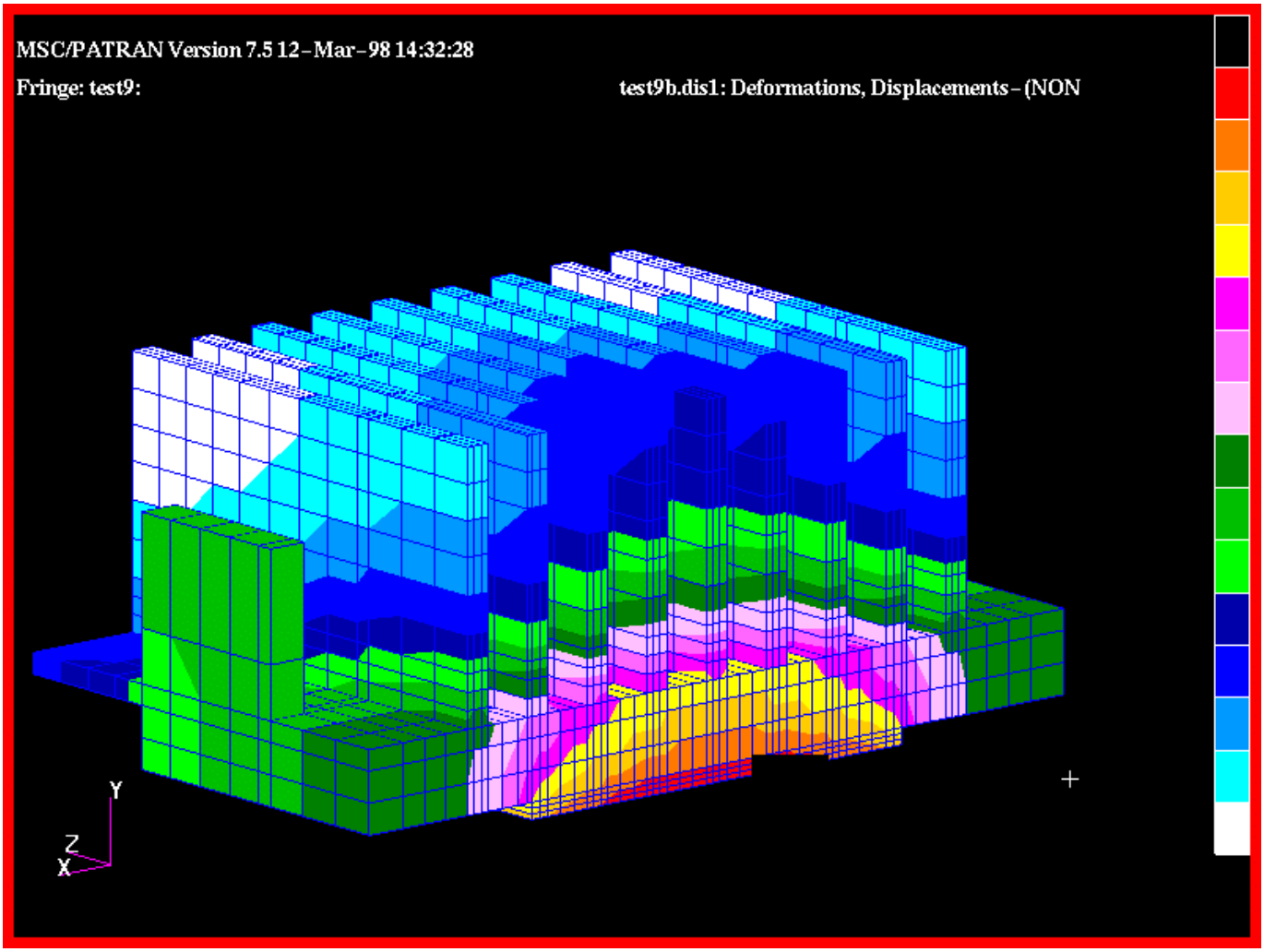

Figure 10: Calculated temperature field of prototype heat sink at 1W applied chip power

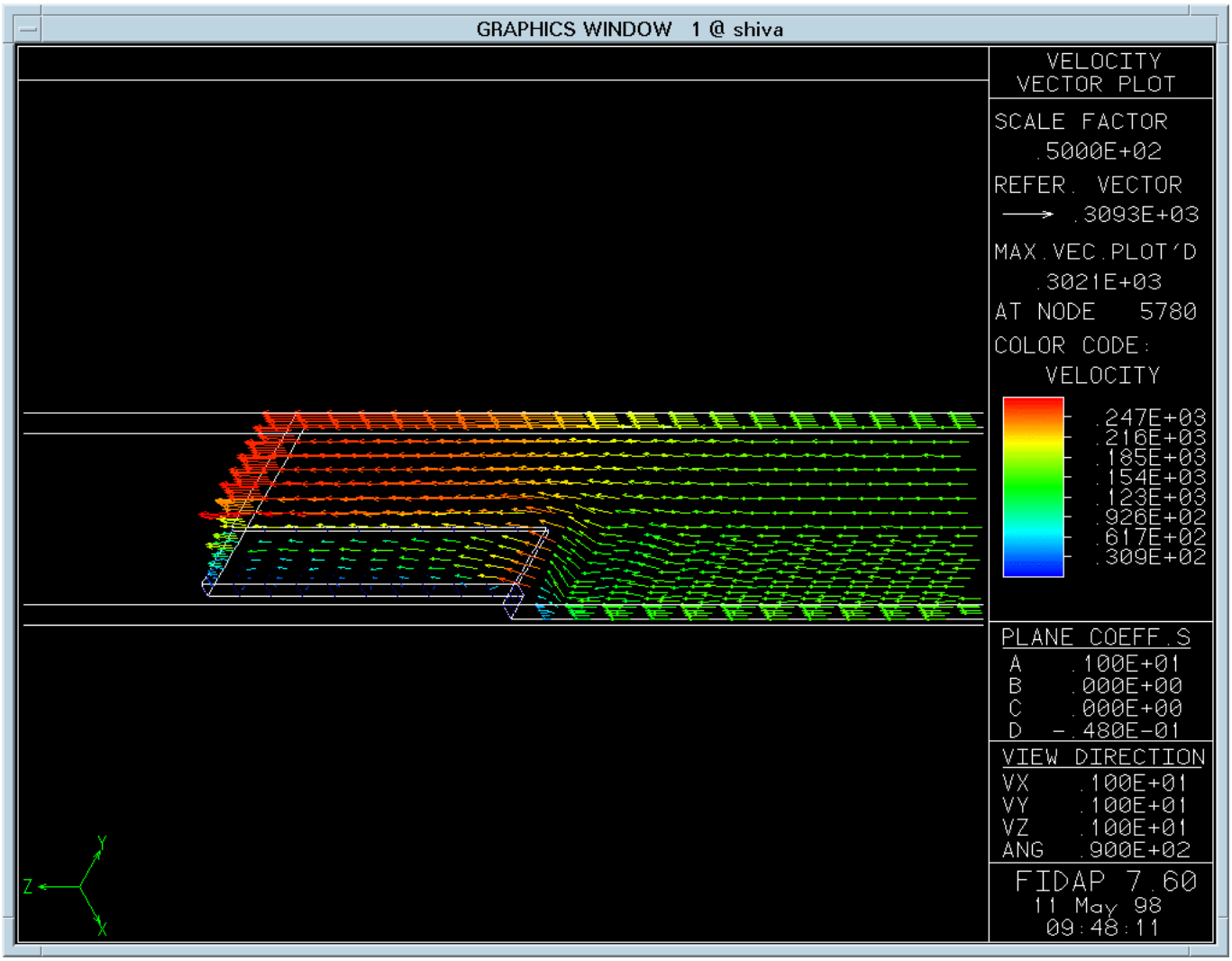

Figure 11: Velocity field computed from FIDAP analysis

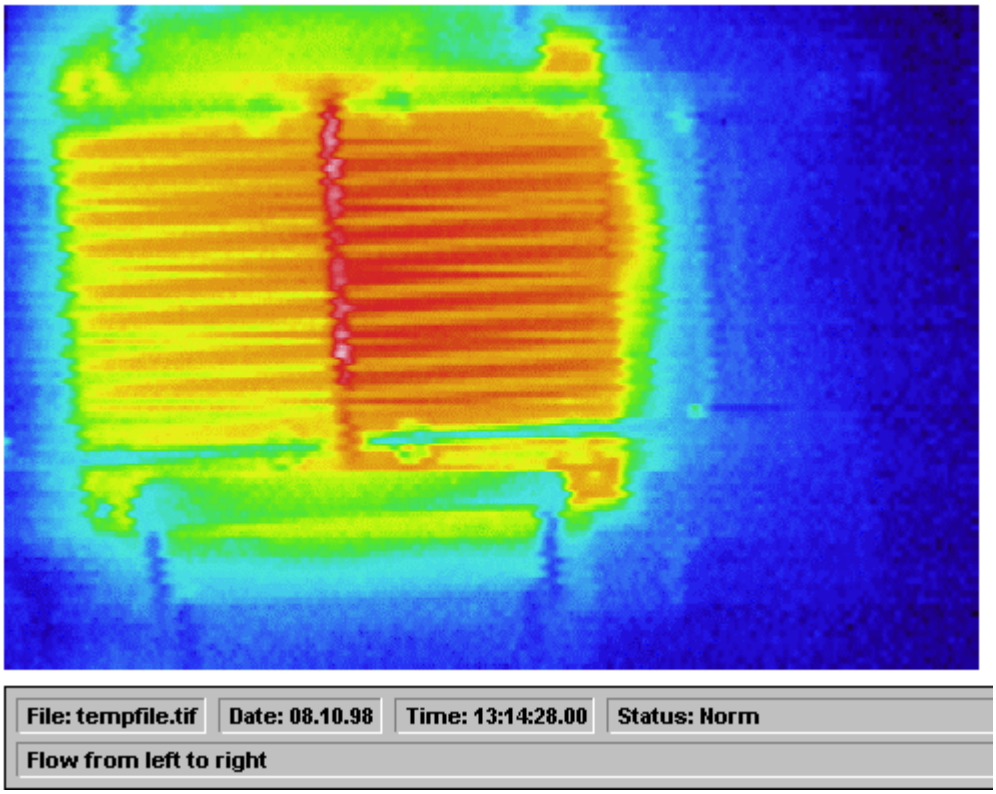

Figure 12a: IR image of BITS heat sink in wind tunnel testing. Airflow is from left to right.

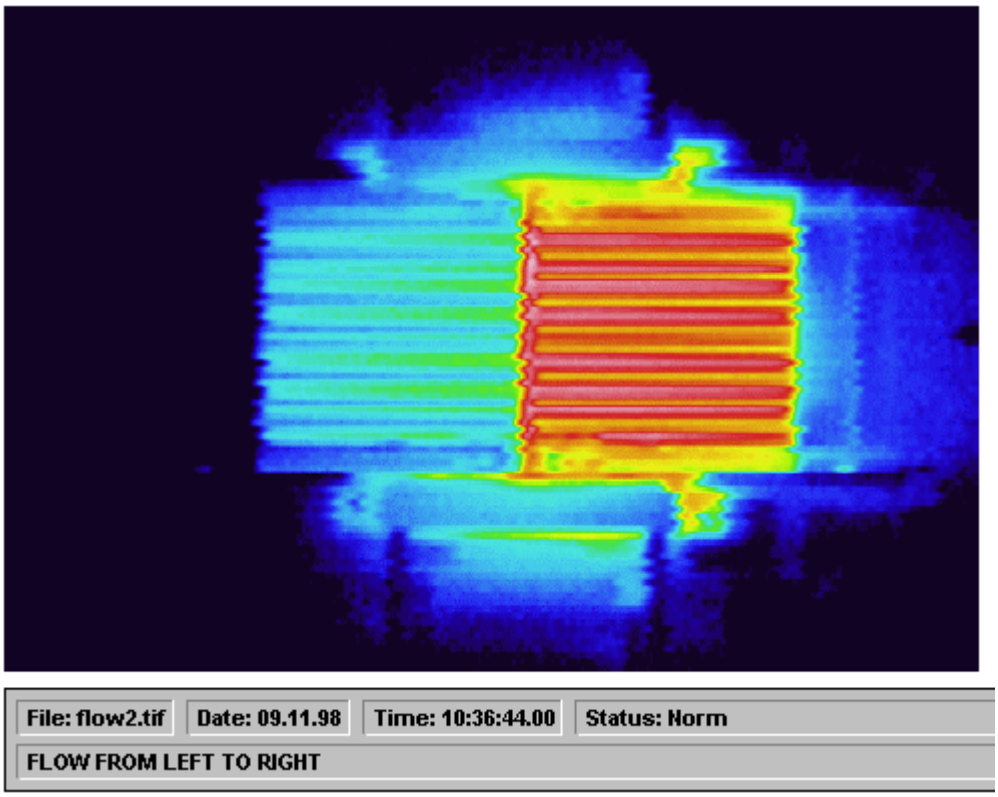

Figure 12b: IR thermograph of BITS heat sink showing inconsistency of interface thermal condition

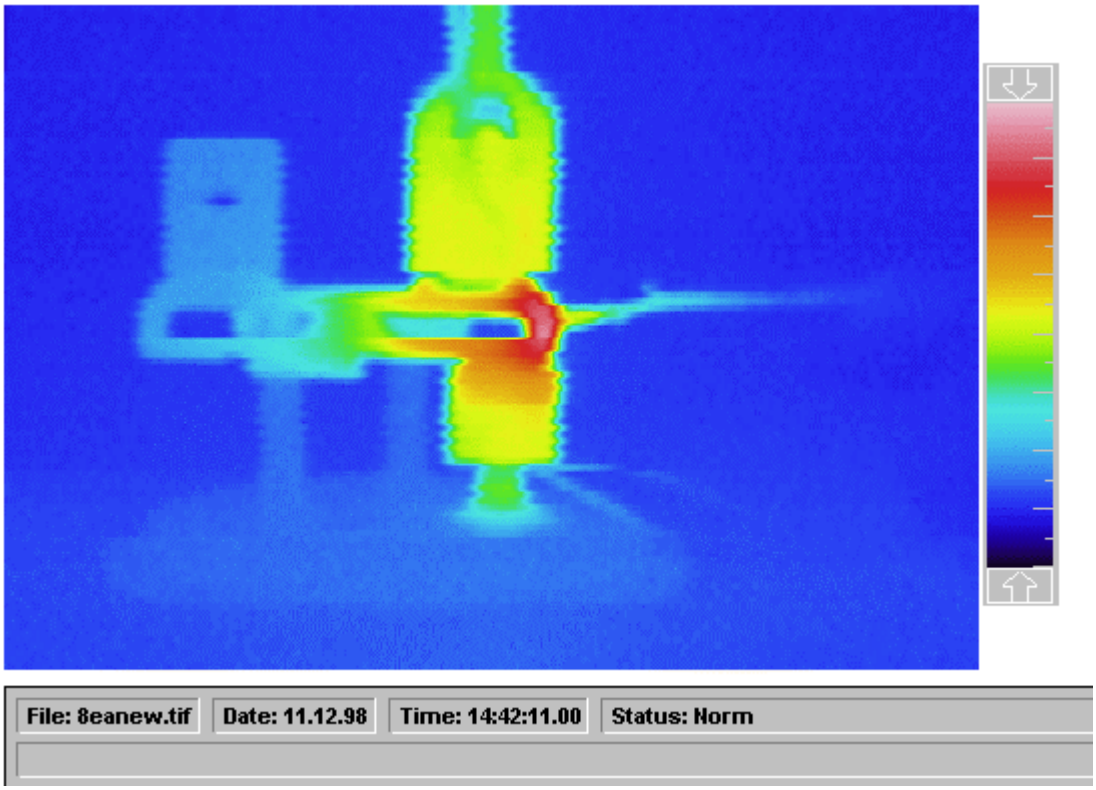

Figure 13: IR thermograph of motor starter terminal assembly

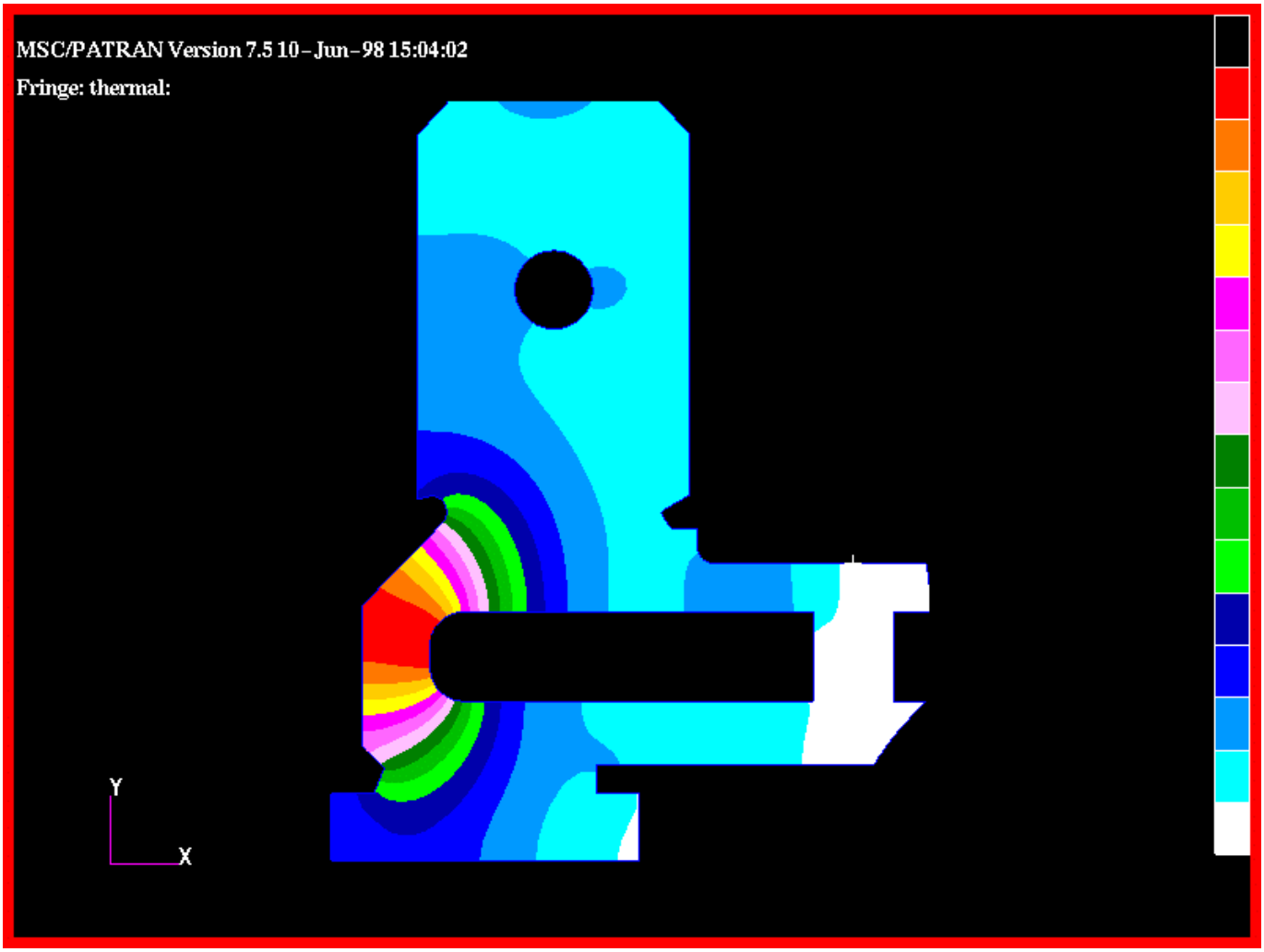

Figure 14: Temperature field from the finite element results

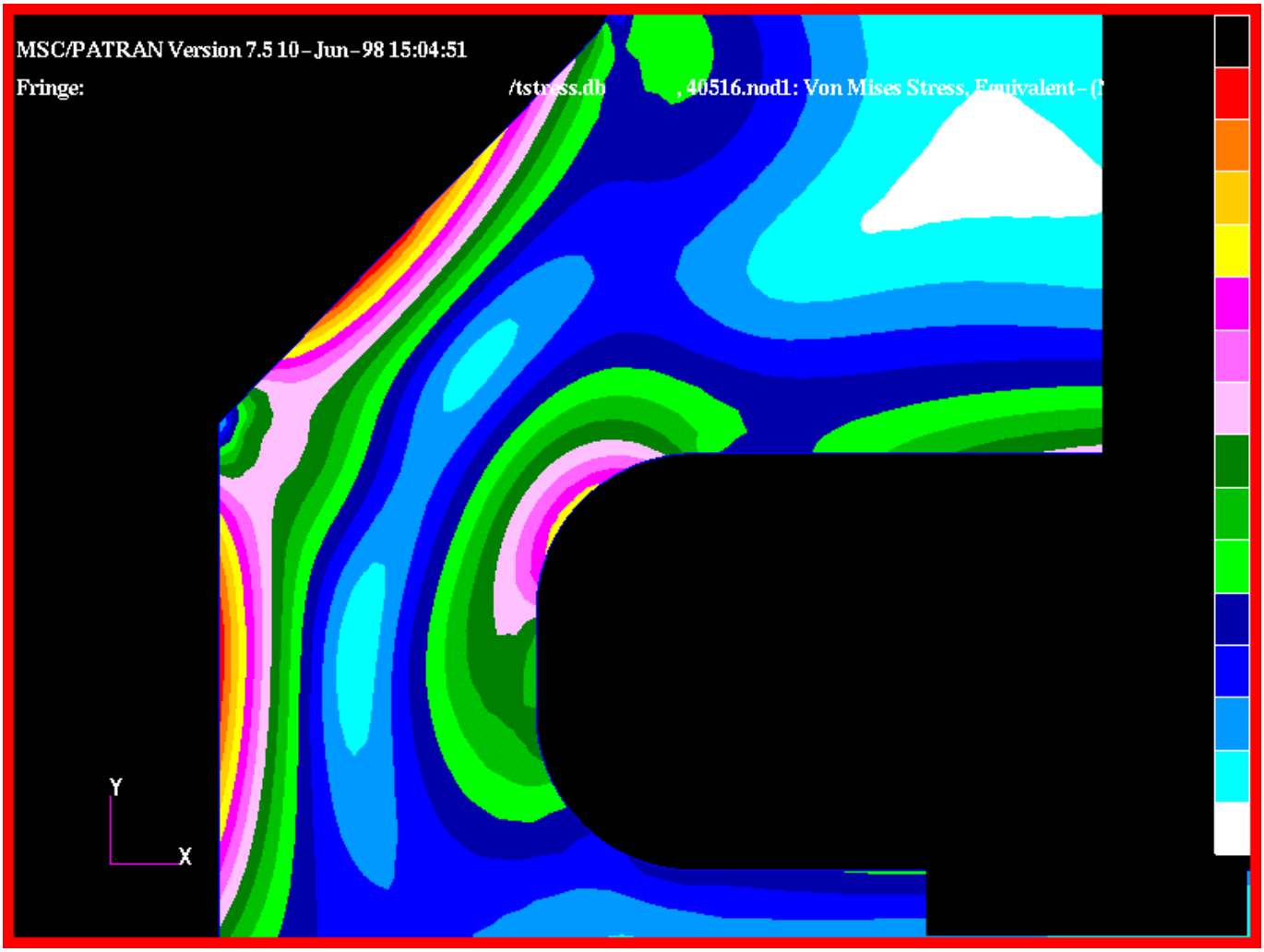

Figure 15: Von Mises stress field induced by thermal transient